How and Why Nanoparticle's Curvature Regulates the Apparent pK_a of the Coating Ligands

Dawei Wang,[†,‡,#] Rikkert J. Nap,[§,||,#] István Lagzi,[‡] Bartlomiej Kowalczyk,[‡] Shuangbing Han,[‡] Bartosz A. Grzybowski,[*,‡,⊥] and Igal Szleifer[*,‡,§,||,⊥]

[†]School of Materials Science and Engineering, Northwestern Polytechnical University, Xi'an 710072, People's Republic of China

[‡]Department of Chemical and Biological Engineering, [§]Department of Biomedical Engineering, [||]Chemistry of Life Processes Institute, and [⊥]Department of Chemistry, Northwestern University, 2145 Sheridan Road, Evanston, Illinois 60208, United States

S Supporting Information

ABSTRACT: Dissociation of ionizable ligands immobilized on nanoparticles (NPs) depends on and can be regulated by the curvature of these particles as well as the size and the concentration of counterions. The apparent acid dissociation constant (pK_a) of the NP-immobilized ligands lies between that of free ligands and ligands self-assembled on a flat surface. This phenomenon is explicitly rationalized by a theoretical model that accounts fully for the molecular details (size, shape, conformation, and charge distribution) of both the NPs and the counterions.
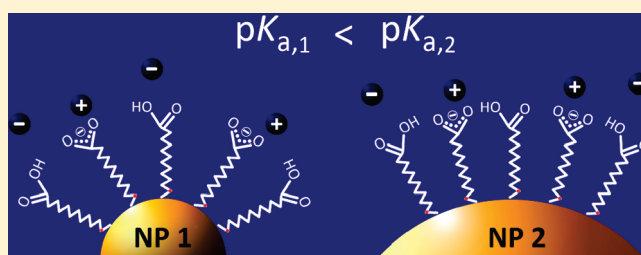
INTRODUCTION

Immobilization of organic molecules onto nanometer-sized particles (NPs) can modify the physicochemical properties of these molecules, including the redox potentials,[1] ability to undergo conformational changes,[2,3] or the assembly of hierarchical structures.[3] Despite numerous experimental studies involving NP-immobilized molecules, however, many aspects of how NP curvature affects the immobilized ligands are poorly understood. In particular, it is unclear how this curvature modifies the acid—base equilibria and the pK_a of the acidic ligands.[4−6] Acid-decorated NPs have been used widely in electrostatic self-assembly of the NP crystals,[7] in the formation of NP coatings,[8] and in Stellacci's striped NPs.[3] In all of these systems, the knowledge of the protonation state of the ligands is crucial for their proper functioning and/or assembly into larger structures. Here, we combine experiments with fundamental theory of the dissociation effects in NPs covered with self-assembled monolayers (SAMs[9,10]) of model acidic ligands, 11-mercaptoundecanoic acid (MUA). The key finding of our work is that the pK_a of the on-particle MUA SAMs depends perceptibly on the NP's radius and differs from the value characterizing the SAM on a flat surface[11,12] by as much as two pH units. In addition, the value of the pK_a can be controlled by the concentration of salt in solution and by the size of the salt's ions. The experimental pK_a trends (determined by acid—base titration[13]) are reproduced by a theoretical model that accounts fully for the molecular details (size, shape, conformation, and charge distribution) of both the NPs and the counterions. The method we describe in this Article can be extended to other types of molecules/NPs[14,15] and can

help tailor the properties of nanostructured materials and systems based on ionizable molecules.[16,17]

EXPERIMENTAL SECTION

Gold nanoparticles, AuNPs (Figure 1a), were synthesized as described preciously[4,16] and had diameters of metal cores in different batches 4.1 ± 0.5, 5.0 ± 0.5, and 7.2 ± 0.8 nm (size distributions and standard deviations were determined from transmission electron microscopy, TEM, images; see Figure 1b and Figure S1 in the Supporting Information). The NPs were functionalized with a SAM of 11-mercaptoundecanoic acid (MUA, ProChimia Surfaces, ultrapure grade; pK_a in solution ∼4.8[18]) as described in ref 7. Upon attachment to the gold surface, one MUA ligand occupied, on average, the area of 21.3 Å^2 (as estimated in ref 4).

The dissociation behavior of NP-tethered MUAs was studied as a function of pH and/or salt concentration using an acid—base (or potentiometric) titration method.[13] In a typical procedure, the pH of 8 mL of AuNP solution of 0.2 mM on-particle MUA ligands was adjusted to ∼9.3 by the addition of tetramethylammonium hydroxide (TMAOH). One 200 mM aliquot of tetramethylammonium chloride (TMACl), tetraethylammonium chloride (TEACl), or tetrabutylammonium chloride (TBACl) was added to the stirred AuNP solution, and 80 μL aliquots of 2 mM HCl were then used to titrate the AuMUA solution. Five minutes after each addition of HCl, the pH was measured by InLab 413, Metler Toledo pH electrode (note: the pH did not change significantly after ∼40 s).
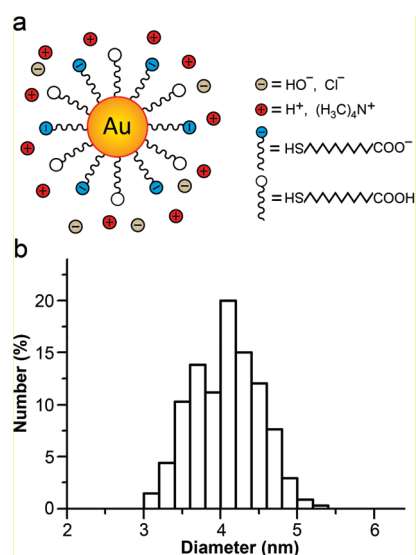
Figure 1. (a) Scheme illustrating dissociation of MUA ligands immobilized on the surface of AuNPs. (b) An example of TEM-derived size distribution of AuMUA NPs. Here, the average diameter of AuNP metal cores is ~4.1 nm; distributions for particles of other sizes are included in Figure S1 in the Supporting Information.

■ EXPERIMENTAL ANALYSIS

For the dissociation of the MUA ligands, $AH \rightleftharpoons H^+ + A^-$, the acid equilibrium/dissociation constant is given by $K_a = \{H^+\}\{A^-\}/\{AH\}$, where $\{i\}$ denotes the activity of species i (in equilibrium at the NPs' surface) and can be approximated by the corresponding concentration of species i when the solution is sufficiently dilute.

For the analysis of the experimental titration data, it is convenient to introduce the fraction of charged MUA ligands on AuNPs (i.e., the degree of dissociation of MUA ligands), $f = [A^-]/([A^-] + [AH])$, where $[AH]$ and $[A^-]$ represent, respectively, the concentrations of the protonated and the deprotonated MUAs on the particles, and $[A^-]$ can be calculated from the charge balance condition, $[H^+] + [TMA^+] = [OH^-] + [Cl^-] + [MUA^-]$, with $[H^+]$ estimated from the experimentally determined pH of the bulk solution. The fraction of charged MUA on the NPs then becomes

$$f = \frac{1}{1 + [H^+]/K_a} \quad (1)$$

and the pK_a of the MUA on the particles can be expressed by the so-called Henderson−Hasselbalch equation, $pK_a = pH - \log[f/(1 - f)]$. Solid markers in Figure 2a show a typical experimental dependence of f on pH for 4.1 nm AuNPs in the solution of 80 mM TMACl. Although this dependence agrees qualitatively with the predictions of the Henderson−Hasselbalch equation (i.e., degree of dissociation increases with pH), the calculated pK_a, shown in the inset, systematically deviates from its expected constant value. Clearly, the assumption of an ideal-solution behavior of the NP-immobilized MUA ligands and the application of Henderson−Hasselbalch are not justified. Therefore, to characterize the dissociation of MUA on NPs, we introduce an apparent pK_a defined as the pH for which the degree of dissociation is $f = 0.5$. This definition will be helpful for summarizing the experimental results and for the comparison with the theoretical model.[19]
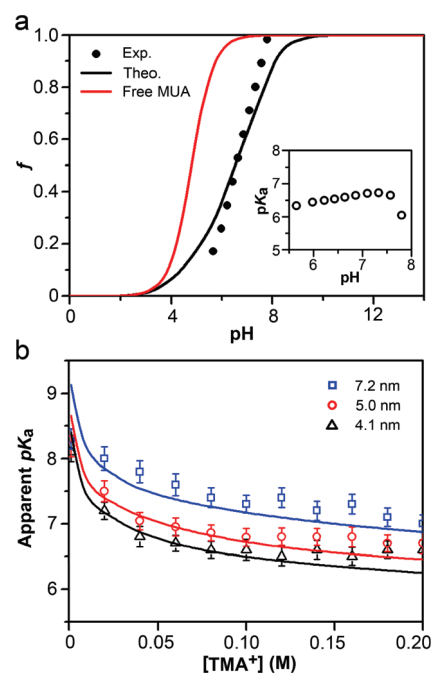
Figure 2. (a) Fractions of charged/dissociated MUA ligands as a function of pH. The theoretical charge fraction (black curve), f, was calculated via eqs 1−9. The red curve is calculated for free MUA in solution using the Henderson−Hasselbalch equation; note that this curve is steeper than both the experimental dependence and the theoretical curve calculated using our theory. The inset shows the experimental pK_a (open markers) of NP's ligands calculated using the Henderson−Hasselbalch equation. Diameter of the NP's metal core, $D(AuNP) = 4.1$ nm, $c(TMACl) = 0.08$ M. (b) The apparent pK_a's of AuMUA NPs of different sizes plotted as a function of salt concentration. Open markers correspond to experimental data; curves were calculated by the model described in the main text.

Figure 2b summarizes the key experimental results of this study and plots the apparent pK_a as a function of salt (TMACl) concentration for AuNPs with three different average diameters: 4.1, 5.0, and 7.3 nm. We note that in all cases, the apparent pK_a of NP-immobilized ligands is significantly higher than the $pK_a \approx 4.8$ of MUA in solution. The apparent pK_a also increases with increasing NP size and decreases with increasing salt concentration (especially for salt concentration $c_s < 0.05$ M).

■ THEORETICAL ANALYSIS

The fact that the fraction of charged MUA on NPs does not follow the ideal-solution behavior prescribed by eq 1 indicates that the degree of dissociation is affected by the restriction/immobilization of the −COOH groups in the dense SAM and, possibly, by other factors such as NP curvature. In reality, as mentioned above, the equilibrium constant should be defined in terms of the activities rather than the concentrations. In many cases, and particularly in dilute solutions, the activity becomes the concentration. However, even for very low concentrations of NP, the local environment of the acid groups determines, through a balance of chemical free energy, electrostatic, van der Waals, steric, and packing interactions, its protonation state. To account for these effects, it is necessary to calculate and minimize the free energy of the system, which explicitly includes the coupling between the chemical equilibrium and all the relevant interactions.

2193

dx.doi.org/10.1021/ja108154a |*J. Am. Chem. Soc.* 2011, 133, 2192–2197

The free energy formalism we use in the following is the first application of our theory[20,21] to nanoparticulate systems. The molecular approach explicitly incorporates the molecular details of each species present in the system including the size, shape, conformation, and charge of every molecule. This theoretical approach has been previously shown to be quite versatile and accurate as compared to experimental observations in various applications,[20,22−27] ranging from the switching properties of poly vinyl pyridine grafted to nanopores[28] to the variation of the properties of grafted poly acrylic acid as a function of pH and solution ionic strength.[25,29]

Here, we apply this theory to model a gold nanoparticle of radius R and covered with σ MUA ligands per unit area ($\sigma \approx 4.7$ nm^{-2} for MUA on AuNPs[30]). The MUA molecules are composed of $n = 13$ segments (including the mercaptoundecyl chain and the ionizable end group −COOH), and each segment has a volume $v_p = 27$ Å^3.[31] The NP is immersed in an aqueous solution, containing monovalent TMACl salt, which is assumed to be completely dissociated. Water is also able to dissociate into protons (H$^+$) and hydroxyl ions (OH$^-$). The bulk solution is characterized by a salt concentration (c) and by bulk pH. The bulk pH is controlled by the addition of extra TMAOH or HCl.

The appropriate free energy to treat a single NP embedded in a solution of a given salt concentration and pH is a semi grand-potential where the number of MUAs on the NP is fixed, and the chemical potential of the mobile species is given by that of the bath, that is, the bulk solution. It is convenient to write the free energy per unit area at the surface of the NP, $A(R)$. Furthermore, due to the spherical symmetry of the NP, we consider inhomogeneities only in the radial direction, r. Thus,

$$\frac{\beta F}{A(R)} = \sigma f \sum_{\alpha = \alpha_{A^-}} P(\alpha) \ln P(\alpha) + \sigma(1-f) \sum_{\alpha = \alpha_{AH}} P(\alpha) \ln P(\alpha)$$

$$+ \beta f \sum_{\alpha = \alpha_{A^-}} P(\alpha_{A^-})\varepsilon(\alpha_{A^-}) + \beta(1-f) \sum_{\alpha = \alpha_{AH}} P(\alpha_{AH})\varepsilon(\alpha_{AH})$$

$$+ \sigma f(\ln f + \beta\mu_{A^-}^\circ) + \sigma(1-f)[\ln(1-f) + \beta\mu_{AH}^\circ]$$

$$+ \beta \int dr\, G(r)\left[\langle\rho_q(r)\rangle\psi(r) - \frac{1}{2}\varepsilon(r)\varepsilon_0(\nabla_r\psi(r))^2\right]$$

$$+ \int dr\, G(r)\rho_w(r)[\ln \rho_w(r)v_w - 1 - \beta\mu_w]$$

$$+ \int dr\, G(r)\rho_+(r)[\ln \rho_+(r)v_w - 1 - \beta\mu_+]$$

$$+ \int dr\, G(r)\rho_-(r)[\ln \rho_-(r)v_w - 1 - \beta\mu_-]$$

$$+ \int dr\, G(r)\rho_{H^+}(r)[\ln \rho_{H^+}(r)v_w - 1 + \beta\mu_{H^+}^\circ - \beta\mu_{H^+}]$$

$$+ \int dr\, G(r)\rho_{OH^-}(r)[\ln \rho_{OH^-}(r)v_w - 1 + \beta\mu_{OH^-}^\circ - \beta\mu_{OH^-}]$$

$$(2)$$

where $\beta = 1/k_BT$ is the inverse absolute temperature. The first two terms in eq 2 represent the conformational entropies of the charged and uncharged MUA ligands, with $P(\alpha)$ being the

probability distribution function (PDF) of finding a ligand in conformation α. The third and the fourth terms represent the average internal energies of the ligands when the carboxylic group is in the deprotonated and protonated state, respectively. The next two terms correspond to the entropies of mixing between the charged and uncharged state of −COOH group of the ligand,[21,32] and also include the standard free energies of formation for the charged and uncharged state (denoted by $\mu_{A^-}^\circ$ and μ_{AH}°, respectively). The seventh term in the free energy expression represents the electrostatic contribution,[33−35] where $\psi(r)$ is the electrostatic potential and $\langle\rho_q(r)\rangle$ is the total charge density given by:

$$\langle\rho_q(r)\rangle = -\sigma f \sum_{\alpha_{A^-}} P(\alpha_{A^-})n^e(\alpha_{A^-};r)e + \rho_+(r)e - \rho_-(r)e$$

$$+ \rho_{H^+}(r)e - \rho_{OH^-}(r)e \quad (3)$$

with the first term corresponding to the average charge of a ligand at position r, where $n^e(\alpha_{A^-};r)\,dr$ is the number of carboxylate groups in conformation α_{A^-} within a concentric "shell" $(r, r + dr)$. The remaining terms account for the charges of the cations (TMA$^+$), anions (Cl$^-$), protons (H$^+$), and hydroxyls (OH$^-$), and e is the unit of charge. In eq 2, $\varepsilon(r)$ stands for a position-dependent relative dielectric constant, which is assumed to be a weighted average of all its components, $\varepsilon(r) = \sum_i \varepsilon_i\phi_i(z)$, where $\phi_i(z)$ is the volume fraction of species i, ε_0 is the permittivity of vacuum, $\varepsilon_p = 3$ for the organic, MUA SAM,[21] and the dielectric constant of the remaining components in solution (i.e., ions and water) is assumed equal to that of water, $\varepsilon_w = 78.5$.

The next five terms in eq 2 represent the mixing (translational) entropy and the bath chemical potentials, μ_i, of all the ions and solvent molecules, where $\rho_i(r)$ is the density of molecules of type i and v_w is the volume of a water molecule.

The intermolecular repulsive interactions are accounted for by local packing constraints; that is, they represent excluded volume interactions. Specifically,

$$\sigma f \sum_{\alpha_{A^-}} P(\alpha_{A^-})n(\alpha_{A^-};r)v_p + \sigma(1-f) \sum_{\alpha_{AH}} P(\alpha_{AH})n(\alpha_{AH};r)v_p$$

$$+ \rho_w(r)v_w + \rho_+(r)v_+ + \rho_-(r)v_- + \rho_{H^+}(r)v_{H^+}$$

$$+ \rho_{OH^-}(r)v_{OH^-} = 1 \quad (4)$$

where v_i is the volume of molecule of type i and $n(\alpha, r)\,dr$ corresponds to the number of segments of the MUA ligand in conformation α within the radial volume contained within r and $r + dr$.

In all the integrals in eq 3, $G(r) = A(r)/A(R) = (r/R)^2$ is a geometrical factor describing the change in volume depending on the distance from the surface.[36]

The functional variation of the free energy with respect to the $P(\alpha)$, f, $\rho_i(r)$, and $\psi(r)$ subject to the packing constraints, eq 4, leads to a set of equations for the probability distribution function (PDF), the degree of dissociation of the MUAs, the densities of the ions (TMA$^+$, H$^+$, Cl$^-$, and OH$^-$) and water molecules, and the electrostatic potential. The PDF is

$$P(\alpha_{AH}) = \frac{1}{q_{AH}} \exp[-\beta \int \pi(r)n(r;\alpha_{AH})v_p\, dr - \beta\varepsilon(\alpha_{AH})]$$

$$\times \exp\left[\frac{\beta}{2} \int n(r;\alpha_{AH})\frac{d\varepsilon(r)\varepsilon_0}{d\langle\phi_{AH}(r)\rangle}(\nabla_r\psi(r))^2\, dr\right]$$

2194

dx.doi.org/10.1021/ja108154a |J. Am. Chem. Soc. 2011, 133, 2192–2197

$$P(\alpha_{A^-}) = \frac{1}{q_{A^-}} \exp\left[-\beta \int n(r; \alpha_{A^-}) \pi(r) \nu_p \, dr - \beta \varepsilon(\alpha_{A^-})\right]$$

$$\times \exp\left[\frac{\beta}{2} \int n(r; \alpha_{A^-}) \frac{d\varepsilon(r)\varepsilon_0}{d\langle\phi_{A^-}(r)\rangle} (\nabla_r \psi(r))^2 \, dr\right]$$

$$\times \exp\left[-\beta \int n^e(r; \alpha_{A^-})(-e)\psi(r) \, dr\right] \quad (5)$$

where $\pi(r)$ is the lateral pressure, which enforces the packing constraints in the PDF $P(\alpha_i)$, eq 5, and q_i is the partition function of species i that ensures the normalization of the PDF, that is, $\sum_{\alpha=\alpha_i} P(\alpha) = 1$. The expression for the degree of dissociation is then

$$\frac{f}{1-f} = \frac{q_{A^-}}{q_{AH}} \exp[-\beta(\mu_{A^-}^\circ - \mu_{AH}^\circ)] \quad (6)$$

Variation of the free energy expression with respect to the electrostatic potential leads to the Poisson equation:

$$\nabla_r(\varepsilon(r)\nabla_r \psi(r)) = -\langle\rho_q(r)\rangle \quad (7)$$

The explicit expressions for the densities are

$$\rho_i(r)\nu_w = \exp[\beta(\mu_i - \mu_i^\circ) - \beta\pi(r)\nu_i - \beta\psi(r)q_i] \quad (8)$$

The unknowns in eqs 5–8 are the lateral pressures and the electrostatic potential. Application of the theory requires evaluating all these variables. This is accomplished by substituting the volume fractions into the incompressibility constraint and the Poisson equation providing a set of integral-differential equations, whose solution determines the lateral pressures and electrostatic potential. In practice, we discretize the space and thereby convert the differential equations into a set of coupled nonlinear equations that are solved numerically.[37] The inputs necessary to solve the equations include the size, shape, and charge of the molecular species, the conformations and distribution of the ionizable units on the ligands (here, the −COOH), and the conditions of the bulk solution, that is, TMACl concentration and the bulk pH. Details concerning the chain model used for the MUA, the discretization, and numerical methodology can be found in section 2 of the Supporting Information and in refs 20–22.

The expression derived for the degree of dissociation, f, involves the difference between the individually unknown standard chemical potentials $\mu_{A^-}^\circ$ and μ_{AH}°. These chemical potentials, however, are related to the free energy of the acid–base reaction (here, the dissociation of MUA, $AH \rightleftharpoons H^+ + A^-$), $\Delta G^\circ = \mu_{A^-}^\circ + \mu_{H^+}^\circ - \mu_{AH}^\circ$, which is in turn related to the acid–base equilibrium constant of a single MUA molecule in dilute solution $K_a = C \exp(-\beta\Delta G^\circ)$, for which we take the value of $pK_a = 4.8$,[18] and C is a constant introduced for consistency of units. The above definition allows us to express the chemical equilibrium equation, eq 6, in terms of the bulk experimental acid–base equilibrium constant as defined in eq 1, yielding the fraction of charged MUA ligands immobilized on AuNPs:

$$f = \frac{1}{1 + \dfrac{q_{AH}}{q_{A^-} q_{H^+}} \dfrac{[H^+]}{K_a}} \quad (9)$$

In deriving the above equation, we also made use of the following relation for the bulk density of the protons,
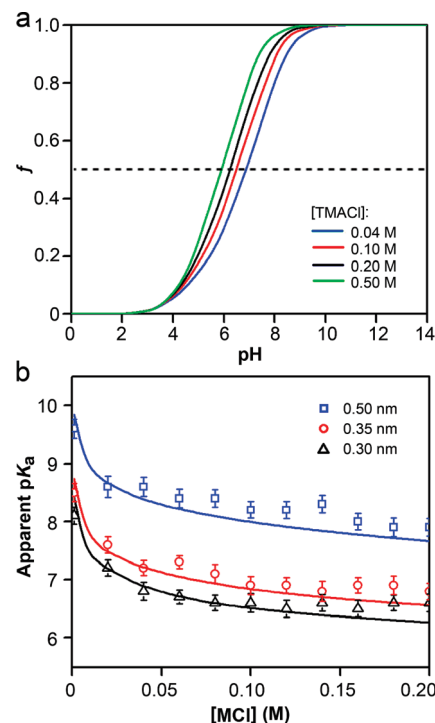
Figure 3. (a) Calculated fractions of dissociated MUAs, f, on 4.1 nm AuNP as a function of bulk pH in solutions with different bulk salt concentrations of TMACl. Dashed line indicates $f = 0.5$. (b) The dependencies of the apparent pK_a of AuMUA NPs on the salt concentration and on the size of the salt cations (here, the anions are always Cl^-). $R = 0.30$, 0.35, and 0.50 nm correspond to the radii of TMA^+, TEA^+, and TBA^+, respectively. D(AuNPs) = 4.1 nm. Open markers correspond to experimental data; curves are calculated on the basis of the model described in the text.

$\rho_{H^+}^{bulk} = \exp(-\beta\mu_{H^+}^\circ)q_{H^+}$, where q_{H^+} is the "partition function" of the protons given by $q_{H^+} = \exp(-\beta\pi_{bulk}\nu_{H^+} - \beta\psi_{bulk}e)$. Equation 9 can be viewed as expressing the nonideality of the NP system because it contains the activities of the molecular species rather than concentrations (cf., eq 1). The partition functions q_{AH}, q_{H^-}, and q_{H^+} describe the nonideal interactions of the species with its environment.[21,38]

Finally, we observe that in our experiments the AuNPs are not monodisperse but have a distribution of sizes. To account for the size polydispersity, a quenched average over the particles sizes was performed. The average degree of dissociation was then determined by computing the degrees of dissociation for different NP radii and weighting them with the appropriate probabilities, $\langle f \rangle = \int dD \, P(D)f(D)$, where D is the diameter of the AuNPs' metal cores, and $P(D)$ is the size distribution function obtained from experiments (cf., Figure 1b and Figure S1 in the Supporting Information). Note that the average can only be performed if the NP solution is sufficiently dilute; that is, the AuNPs do not interact with each other, which is a central assumption of our theory because the molecular theory, in the form used here, treats one NP that interacts with the solution.

■ RESULTS AND DISCUSSION

On the basis of the above discussion, the fraction of charged MUA ligands on AuNPs can be calculated without any adjustable fitting parameters (cf., Figure 3a for the fraction of the charged MUA on 4.1 nm AuNPs), from which the apparent pK_a can be

2195

dx.doi.org/10.1021/ja108154a |J. Am. Chem. Soc. 2011, 133, 2192–2197

determined. The theoretical results agree well with the experimental ones, as was convincingly demonstrated in Figures 2b and 3b. Both theoretical modeling and experimental observations show that the fraction of the charged ligands on AuNPs (1) increases with the increasing pH of the bulk solution, (2) decreases with decreasing salt concentration (for given NP size and pH), (3) decreases with increasing NP size, and therefore (4) the apparent pK_a determined from $f_{1/2}$ increases with increasing NP size. These trends are rationalized below.

Upon decreasing salt concentration, the electrostatic repulsions between the charged carboxylate groups ($-COO^-$) become stronger, as the charges are less shielded. Therefore, it is an energetically unfavorable process. The system has two options to alleviate these large energetic repulsions. The first possibility is to bring extra counterions (e.g., TMA^+) from the bulk solution at the penalty of reducing their entropy. The second option involves shifting the acid—base equilibrium toward the uncharged state, that is, decreasing the amount of charged MUA ligands. The free energy cost of reducing the amount of charge equals the free energy of the deprotonation of the acid group, ΔG°, which for weak acids such as carboxylic is less costly than the counterion confinement.[21] Hence, the decrease in the salt concentration in bulk solution can significantly shift the dissociation equilibrium of MUA toward the energetically more favorable state of protonated MUA ligands, and therefore decreases the fraction of charged MUA ligands, which ultimately results in an increasing apparent pK_a. Also, we predict that the fraction of the charged MUA ligands on AuNPs can be significantly affected by the concentration of TMACl if the pH ranges from ~4 to ~9 (cf., Figure 3a). At pH < 4, the NPs are more than 95% protonated, and thus AuNPs aggregate and precipitate due to van der Waals attractions. For pH > 9, most of the ligands are charged regardless of the salt concentration. In this limit, the interparticle interactions will be modified by the salt concentration, but this is beyond the present study.

Regarding the dependence of the apparent pK_a on the size/curvature of AuNPs, we explain it as follows. As the size of the NP increases, its curvature decreases, and the average distance between the head-groups of deprotonated MUAs decreases. Therefore, the ligands experience stronger electrostatic repulsions. Similar to the salt dependence, the system will respond to this energetically unfavorable situation by "regulating" the ligands' charges by shifting the acid—base equilibrium toward the protonated state. Consequently, the fraction of charged MUA ligands decreases and the apparent pK_a increases with increasing NP size. An interesting corollary here is that the apparent pK_a of the MUAs on AuNPs should lie between the pK_a of free MUA molecules in solution ($pK_a \approx 4.8$) and the apparent pK_a of MUAs within a monolayer on a flat gold surface (apparent $pK_a \approx 10^{11,12}$). We note that while our theory shows quantitative agreement with the experimental data for small NPs ($D < 8$ nm, Figure 2b), discrepancies for larger NPs ($\langle D \rangle = 8.6$ nm) are quite substantial (see the Supporting Information, Figure S2), likely due to the aggregation of such NPs at low pH induced by the strong van der Waals attractions.[30] Also, for the larger size of NP, the disagreement between the experimental observations and the predictions suggests that the charge regulation on the NPs depends on interparticle distance; that is, the apparent pK_a is expected to depend on NP density.

Finally, using our model, we considered the effects of ion size. Figure 3b summarizes the predictions (solid curves) and experimental results (open markers) for titrations involving three salts, TMACl, TEACl, and TBACl, having the same anion, Cl^-, but different cations. The radii of these cations are $R = 0.30, 0.35$, and

0.50 nm[39,40] for, respectively, TMA^+, TEA^+, and TBA^+. As seen, the theory predicts and the experiments confirm that the apparent pK_a increases with increasing size of cations. With increasing ion size, the excluded volume interactions[21] between the ion and the NP ligands increase, and there is a larger free energy cost associated with the localization of the counterions to the SAM layer. As a result, the density of counterions in the vicinity of the charges from the SAM decreases, resulting in stronger electrostatic repulsions between charged MUA headgroups. Increasing the electrostatic repulsions leads to a decrease in the ionization fraction of the MUA, which translates into an increase in the apparent pK_a.

Finally, we note that, although the focus of the present work has been on describing the dissociation behavior of the MUA ligands, our theoretical approach can quantify other structural or thermodynamic quantities pertinent to the system, for example, the spatial distributions of H^+, OH^-, co-, or counterions. Interestingly, the model predicts the variation of pH with the distance from the NP surface, with the value being one to two units lower closer to the NP surface than in the solution's bulk. This difference is expected to increase with increasing particle size, bulk pH, and decreasing salt concentration. Such pH variations should be considered when designing NP—biomolecule conjugates, where the activity of the biocomponent (e.g., an enzyme) can depend on local pH, or in systems of nanocapsules for controlled drug delivery and/or release.

■ CONCLUSIONS

In summary, we described and explained, to our best knowledge, for the first time, the effects of NP curvature/size, ion concentration, and ion size on the apparent pK_a of nanoparticle-immobilized ligands. Our theoretical model incorporates explicitly the molecular details of each species present in the NP/SAM/salt system and reproduces accurately the experimental data without any adjustable/fitting parameters. The results of this work appear crucially important for understanding the details of charge regulation[30,41,42] in nanoparticulate systems. In a wider context, the union of theory and experiments provides a sensitive and accurate tool for the "rational" design of nanoparticles whose charge and solution stability depend on particle size and on the properties of the surrounding medium.

■ ASSOCIATED CONTENT

ⓢ Supporting Information. Size distributions of 5.0 ± 0.5 and 7.2 ± 0.8 nm nanoparticles, and details of the computational methods used (discretization and numerical methodology, the chain model). This material is available free of charge via the Internet at http://pubs.acs.org.

■ AUTHOR INFORMATION

Corresponding Author
grzybor@northwestern.edu; igalsz@northwestern.edu

Author Contributions
#These authors contributed equally.

■ ACKNOWLEDGMENT

(to B.A.G.), and the Nonequilibrium Energy Research Center, which is an Energy Frontier Research Center funded by the U.S. Department of Energy, Office of Science, Office of Basic Energy Sciences under Award Number DE-SC0000989.

■ REFERENCES

(1) Klajn, R.; Olson, M. A.; Wesson, P. J.; Fang, L.; Coskun, A.; Trabolsi, A.; Soh, S.; Stoddart, J. F.; Grzybowski, B. A. *Nat. Chem.* **2009**, *1*, 733.

(2) Klajn, R.; Bishop, K. J. M.; Grzybowski, B. A. *Proc. Natl. Acad. Sci. U.S.A.* **2007**, *104*, 10305.

(3) DeVries, G. A.; Brunnbauer, M.; Hu, Y.; Jackson, A. M.; Long, B.; Neltner, B. T.; Uzun, O.; Wunsch, B. H.; Stellacci, F. *Science* **2007**, *315*, 358.

(4) Kalsin, A. M.; Kowalczyk, B.; Wesson, P.; Paszewski, M.; Grzybowski, B. A. *J. Am. Chem. Soc.* **2007**, *129*, 6664.

(5) Pengo, P.; Baltzer, L.; Pasquato, L.; Scrimin, P. *Angew. Chem.* **2007**, *119*, 404.

(6) Simard, J.; Briggs, C.; Boal, A. K.; Rotello, V. M. *Chem. Commun.* **2000**, 1943.

(7) Kalsin, A. M.; Fialkowski, M.; Paszewski, M.; Smoukov, S. K.; Bishop, K. J. M.; Grzybowski, B. A. *Science* **2006**, *312*, 420.

(8) Smoukov, S. K.; Bishop, K. J. M.; Kowalczyk, B.; Kalsin, A. M.; Grzybowski, B. A. *J. Am. Chem. Soc.* **2007**, *129*, 15623.

(9) Witt, D.; Klajn, R.; Barski, P.; Grzybowski, B. A. *Curr. Org. Chem.* **2004**, *8*, 1763.

(10) Love, J. C.; Estroff, L. A.; Kriebel, J. K.; Nuzzo, R. G.; Whitesides, G. M. *Chem. Rev.* **2005**, *105*, 1103.

(11) Kakiuchi, T.; Iida, M.; Imabayashi, S.; Niki, K. *Langmuir* **2000**, *16*, 5397.

(12) Leopold, M. C.; Bowden, E. F. *Langmuir* **2002**, *18*, 2239.

(13) Albert, A.; Serjeant, E. P. *Ionization Constants of Acids and Bases*; Methuen & Co Ltd.: London, 1962.

(14) Shan, J.; Tenhu, H. *Chem. Commun.* **2007**, 4580.

(15) Pellegrino, T.; Kudera, S.; Liedl, T.; Muñoz Javier, A.; Manna, L.; Parak, W. J. *Small* **2005**, *1*, 48.

(16) Kalsin, A. M.; Grzybowski, B. A. *Nano Lett.* **2007**, *7*, 1018.

(17) Lattuada, M.; Hatton, T. A. *J. Am. Chem. Soc.* **2007**, *129*, 12878.

(18) Sugihara, K.; Teranishi, T.; Shimazu, K.; Uosaki, K. *Electrochemistry* **1999**, *67*, 1172.

(19) The apparent pK_a is not a true equilibrium constant as it is equal to the chemical reaction quotient under the restriction that the degree of dissociation is 0.5. However, for an ideal solution, the apparent pK_a will coincide with the true equilibrium constant.

(20) Szleifer, I.; Carignano, M. A. *Macromol. Rapid Commun.* **2000**, *21*, 423.

(21) Nap, R.; Gong, P.; Szleifer, I. *J. Polym. Sci., Part B: Polym. Phys.* **2006**, *44*, 2638.

(22) Szleifer, I.; Carignano, M. A. *Adv. Chem. Phys.* **1996**, *94*, 165.

(23) Satulovsky, J.; Carignano, M. A.; Szleifer, I. *Proc. Natl. Acad. Sci. U.S.A.* **2000**, *97*, 9037.

(24) Shvartzman-Cohen, R.; Nativ-Roth, E.; Baskaran, E.; Levi-Kalisman, Y.; Szleifer, I.; Yerusalmi-Rozen, R. *J. Am. Chem. Soc.* **2004**, *126*, 14850.

(25) Gong, P.; Wu, T.; Genzer, J.; Szleifer, I. *Macromolecules* **2007**, *40*, 8765.

(26) Wu, T.; Genzer, J.; Gong, P.; Szleifer, I.; Vlček, P.; Šubr, V. *Polymer Brushes*; Wiley-VCH: Weinheim, Germany, 2004; p 287.

(27) Tagliazucchi, M.; Calvo, E. J.; Szleifer, I. *Langmuir* **2008**, *24*, 2869.

(28) Tagliazucchi, M.; Azzaroni, O.; Szleifer, I. *J. Am. Chem. Soc.* **2010**, *132*, 12404.

(29) Wu, T.; Gong, P.; Szleifer, I.; Vlček, P.; Šubr, V.; Genzer, J. *Macromolecules* **2007**, *40*, 8756.

(30) Bishop, K. J. M.; Wilmer, C. E.; Soh, S.; Grzybowski, B. A. *Small* **2009**, *5*, 1600.

(31) Tanford, C. *The Hydrophobic Effect: Formation of Micelles and Biological Membranes*, 2nd ed.; Wiley: New York, 1980.

(32) Raphael, E.; Joanny, J. F. *Europhys. Lett.* **1990**, *13*, 623.

(33) Croze, O. A.; Cates, M. E. *Langmuir* **2005**, *21*, 5627.

(34) Schwinger, J.; DeRaad, J., L. L.; Milton, K. A.; Tsai, W. Y. *Classical Electrodynamics*; Persus Books: Reading, MA, 1998.

(35) Landau, L. D.; Lifshitz, E. M. *Electrodynamics of Continuous Media*; Pergamon Press: Oxford, NY, 1960.

(36) Carignano, M. A.; Szleifer, I. *J. Chem. Phys.* **1995**, *102*, 8662.

(37) Hindmarsh, A. C.; Brown, P. N.; Grant, K. E.; Lee, S. L.; Serban, R.; Shumaker, D. E.; Woodward, C. S. *ACM Trans. Math. Softw.* **2005**, *31*, 363.

(38) Longo, G.; Szleifer, I. *Langmuir* **2005**, *21*, 11342.

(39) Laaksonen, T.; Ahonen, P.; Johans, C.; Kontturi, K. *ChemPhysChem* **2006**, *7*, 2143.

(40) Lok, B. M.; Cannan, T. R.; Messina, C. A. *Zeolites* **1983**, *3*, 282.

(41) Carnie, S. L.; Chan, D. Y. C.; Gunning, J. S. *Langmuir* **1994**, *10*, 2993.

(42) Bishop, K. J. M.; Grzybowski, B. A. *ChemPhysChem* **2007**, *8*, 2171.

2197

dx.doi.org/10.1021/ja108154a |*J. Am. Chem. Soc.* 2011, 133, 2192–2197